

LETTERS

Ancient animal microRNAs and the evolution of tissue identity

Foteini Christodoulou¹, Florian Raible^{1,2,†}, Raju Tomer¹, Oleg Simakov¹, Kalliopi Trachana², Sebastian Klaus^{1,†}, Heidi Snyman¹, Gregory J. Hannon³, Peer Bork² & Detlev Arendt¹

The spectacular escalation in complexity in early bilaterian evolution correlates with a strong increase in the number of microRNAs^{1,2}. To explore the link between the birth of ancient microRNAs and body plan evolution, we set out to determine the ancient sites of activity of conserved bilaterian microRNA families in a comparative approach. We reason that any specific localization shared between protostomes and deuterostomes (the two major superphyla of bilaterian animals) should probably reflect an ancient specificity of that microRNA in their last common ancestor. Here, we investigate the expression of conserved bilaterian microRNAs in *Platynereis dumerilii*, a protostome retaining ancestral bilaterian features^{3,4}, in *Capitella*, another marine annelid, in the sea urchin *Strongylocentrotus*, a deuterostome, and in sea anemone *Nematostella*, representing an outgroup to the bilaterians. Our comparative data indicate that the oldest known animal microRNA, miR-100, and the related miR-125 and let-7 were initially active in neurosecretory cells located around the mouth. Other sets of ancient microRNAs were first present in locomotor ciliated cells, specific brain centres, or, more broadly, one of four major organ systems: central nervous system, sensory tissue, musculature and gut. These findings reveal that microRNA evolution and the establishment of tissue identities were closely coupled in bilaterian evolution. Also, they outline a minimum set of cell types and tissues that existed in the protostome–deuterostome ancestor.

Deep sequencing of *Platynereis* small RNAs identified 34 microRNA families common to protostomes and deuterostomes (Supplementary Fig. 1, Supplementary Table 1), in accordance with recent studies². To investigate the temporal and spatial localization profile of these conserved bilaterian microRNAs, whole mount *in situ* hybridization (WMISH) was conducted using locked nucleic acids as probes. In all cases, localization of mature *Platynereis* microRNAs was spatially restricted and almost exclusively occurred in actively differentiating tissues (Supplementary Fig. 2). We also analysed tissue-specific expression of predicted targets (Supplementary Fig. 3 a, b and Supplementary Table 2) and identified a subset of tissues in which microRNAs were less frequently co-expressed with their predicted targets than expected to occur by chance, whereas other tissues showed the opposite trend (Supplementary Table 3 a, b and Supplementary Data), indicating different modes of involvement of the conserved bilaterian microRNAs in regulating the establishment and/or maintenance of tissue identity⁵.

We found the oldest conserved microRNA, miR-100, shared by cnidarians and bilaterians^{1,2}, highly specifically localized in two small groups of cells of the larval foregut (Fig. 1a, e). These cells also expressed let-7 (Fig. 1b, f) and miR-125 (Fig. 1c), which play a conserved role in developmental timing^{6–8}, and miR-375 (Fig. 1d), demarcating foregut-related, neurosecretory/endocrine cell populations of vertebrate pituitary and pancreas⁹. Marker gene analysis revealed that these cells are

differentiated secretory neurons (Supplementary Fig. 4c). As in fly^{7,8}, *Platynereis* miR-100 and let-7 are processed from a single polycistronic transcript (Supplementary Table 4) that in many bilaterians also includes miR-125 (refs 7,8). Since miR-100, miR-125 and let-7 are expressed much more broadly in fly⁸ and vertebrate¹⁰ (Supplementary Table 5), we challenged evolutionary conservation of the highly specific *Platynereis* pattern by investigating the expression of miR-100 in a cnidarian, the sea anemone *Nematostella*. miR-100 was exclusively detected in single cells located around the pharynx anlage (Fig. 1g and Supplementary Fig. 5a, b), demarcated by *brachyury*¹¹ and *foxa* expression (blue, red and yellow in Fig. 1h). Intriguingly, miR-100, *brachyury*¹² and *foxa2* also colocalize in the *Platynereis* foregut (Fig. 1i; blue, red and yellow in Fig. 1j). These findings indicate that early in animal evolution miR-100 was active in a small population of cells located around a digestive opening. This expression was inherited by let-7 and by miR-125 once they evolved in the bilaterian stem line, to expand into other tissues only later in evolution. Corroborating this, expression of miR-100, miR-125 and let-7 was similarly restricted to foregut tissue in *Capitella* (Fig. 1k, data not shown) and in the sea urchin *Strongylocentrotus* (Fig. 1l and Supplementary Fig. 5c, e).

Locomotor ciliary bands are characteristic for the swimming larvae of marine protostomes and deuterostomes¹³. In *Platynereis*, miR-29, miR-34 and miR-92 demarcated the ciliary bands from early larval stages onwards (Fig. 2a–f) and were also detected in motile ciliated cells of the apical organ and later in the medial head region (Fig. 2a–e). While expression was similar for all ‘ciliary’ microRNAs at early larval stages, partly complementary patterns were observed in the developing young worm (arrowheads in Fig. 2d, e). *Capitella* showed a similar localization of these microRNAs to ciliary bands (Fig. 2h and Supplementary Fig. 6a, b). We also investigated the sea urchin pluteus larva and indeed found miR-92 expressed in the ciliary bands (Fig. 2i) and miR-92 and miR-34 in motile ciliated cells lining the foregut and stomach (Supplementary Fig. 5g, h). The similar specific affiliation of these microRNAs to motile ciliated cells in both protostome and deuterostome larvae is best explained by evolutionary conservation.

Two sets of conserved bilaterian microRNAs showed localized expression in distinct parts of the brain. For miR-7 (ref. 4), miR-137 and miR-153 we observed very similar expression in the dorso-medial neurosecretory tissue of the *Platynereis* brain (Fig. 3a–d) comprising differentiated vasotocinergic and FMRFamide⁴ as well as serotonergic neurons (Fig. 3e). The same microRNAs showed brain-restricted expression in *Capitella* (Supplementary Fig. 6c–e) and have also been reported to show spatially localized expression in the zebrafish brain, including neurosecretory brain parts of the hypothalamus¹⁴ (Supplementary Table 5). Our comparative data thus indicate that these three microRNAs co-evolved in neurosecretory brain tissue. A

¹Developmental Biology Unit, ²Computational Biology Unit, European Molecular Biology Laboratory, D-69117 Heidelberg, Germany. ³Cold Spring Harbor Laboratory, 1 Bungtown Road, Cold Spring Harbor, New York 11724, USA. [†]Present addresses: Max F. Perutz Laboratories, Campus Vienna Biocenter, Dr. Bohr-Gasse 9/4, A-1030 Vienna, Austria (F.R.); J. W. Goethe - Universität Frankfurt Biologie-Campus, Siesmayerstrasse 70-72, D-60323 Frankfurt, Germany (S.K.).

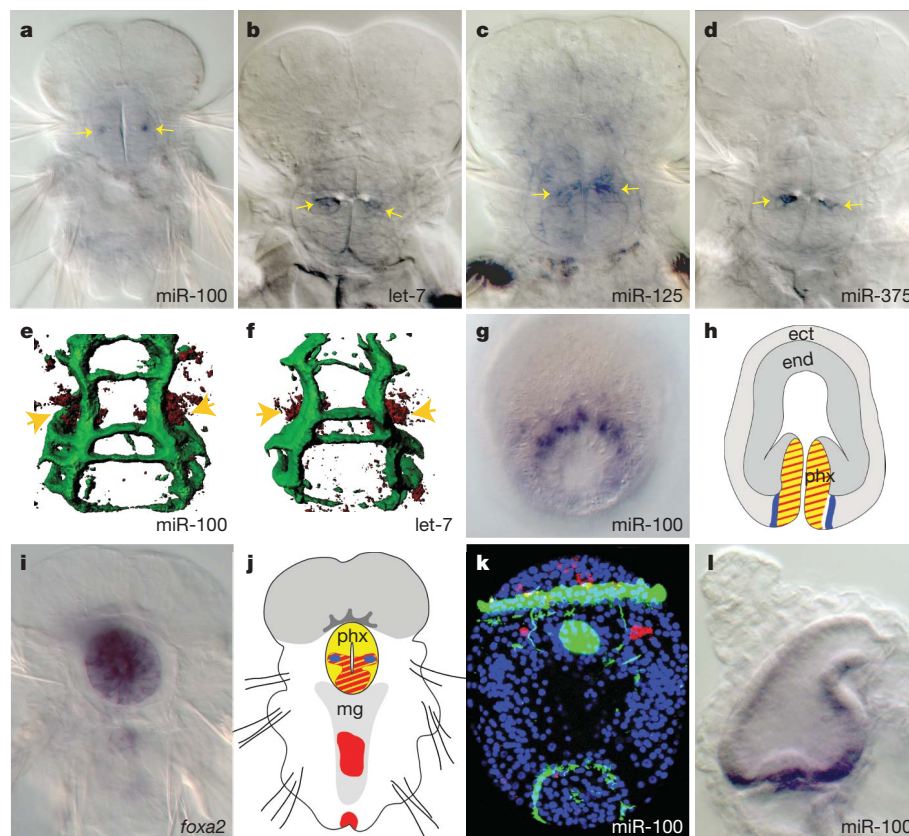
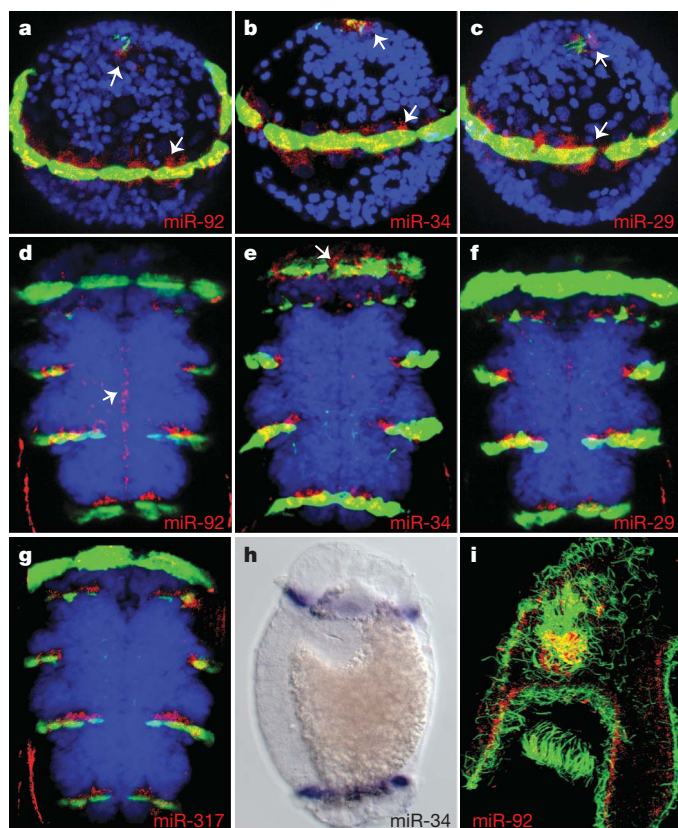


Figure 1 | Foregut-related expression of conserved microRNAs. **a**, Ventral view of 72 hours post fertilization (h.p.f.) *Platynereis*. **b–d**, dorsal view of 5 d.p.f. *Platynereis*. **e**, **f**, Three-dimensional reconstructions of 5 d.p.f. foregut (acTub green, miR-100 and let-7 red). **g**, Oral view of *Nematostella* planula. **h**, Scheme of *Nematostella* planula with pharynx showing *brachyury*¹¹ (red) *foxa*¹¹ (yellow) and miR-100 (blue) expression (phx,

pharynx; end, endoderm; ect, ectoderm). **i**, Ventral view of 72 h.p.f. *Platynereis*. **j**, scheme of 72 h.p.f. *Platynereis* foregut expressing *foxa* (yellow), *brachyury*¹² (red) and miR-100 (blue). **k**, Ventral view of *Capitella* stage 4 larva with expression lateral to stomodaeum and in brain. **l**, Lateral view of *Strongylocentrotus* with expression in sphincter between oesophagus/ stomach.



conserved pair of complementary microRNAs, miR-9 and miR-9*/miR-131 (ref. 15) also showed highly restricted expression in the annelid brain, in two ventro-lateral sets of differentiated neurons (Fig. 3f–h and Supplementary Fig. 6f). In mouse, miR-9 and miR-9*/miR-131 are detected broadly in neuronal precursors but among all differentiated neurons are expressed only in the telencephalon¹⁵, comprising olfactory brain centres. In *Platynereis*, the most apical cells expressing mature miR-9 and miR-9* were located at the base of the antennae, a pair of head appendages considered to be chemosensory sense organs (Fig. 3h). This indicates that miR-9 and miR-9* may ancestrally locate to neurons involved in olfactory/chemosensory information processing. As in vertebrates, both miR-9 and miR-9* are detected in relatively high abundance in *Platynereis* and thus represent a pair of complementary microRNAs conserved in bilaterians².

Other conserved bilaterian microRNAs were expressed more broadly in one of four major organ systems, representing the central nervous system, peripheral sensory tissue, musculature or gut. For each of these groups, expression of individual microRNAs was largely overlapping, but at the same time complementary to those of other groups.

Figure 2 | MicroRNAs expressed in locomotor ciliated cells. **a–c**, Ventral-anterior views of 24 h.p.f. *Platynereis* trochophora larvae with microRNA expression (red) in prototroch cells and apical organ (arrowheads) (blue, DAPI; green, acTub). **d**, Ventral view of 72 h.p.f. *Platynereis* with expression in ciliated cells and midline (arrow). **e**, 72 h.p.f. *Platynereis*; expression in ciliated cells of trunk and prototroch (arrow). **f**, **g**, 72 h.p.f. *Platynereis*; expression in ciliated cells of the trunk. **h**, Lateral view of *Capitella* stage 6 larva; expression in ciliated bands. **i**, Ventral-lateral view of *Strongylocentrotus* pluteus larva with expression in ciliated cells lining the foregut and arms.

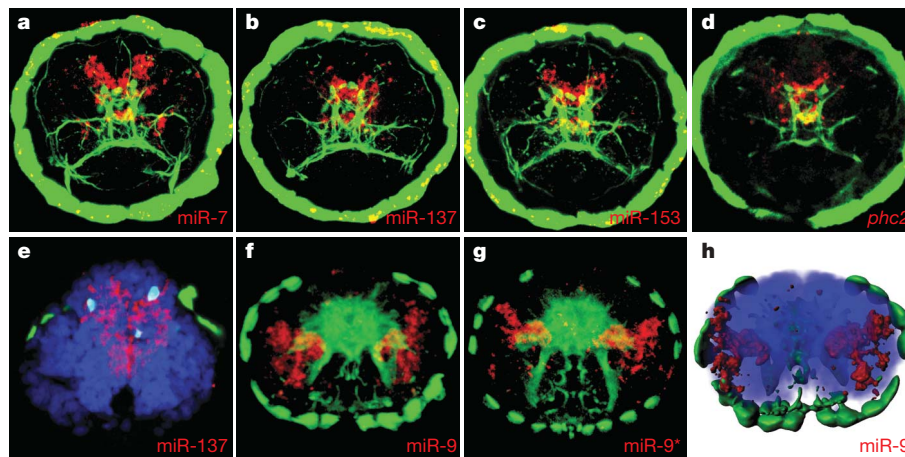


Figure 3 | Expression of brain-specific microRNAs. **a–d**, Apical view of 48 h.p.f. *Platynereis* with expression in dorso-medial brain (green, acTub; red, microRNAs). **e**, Apical view of 72 h.p.f. *Platynereis* brain section showing colocalization of microRNA (red) with serotonin (cyan) (blue,

DAPI, green, acTub). **f, g**, Apical views of 5 d.p.f. *Platynereis* brain. **h**, 3D reconstruction of 5 d.p.f. apical brain with superficial expression at the base of antennae.

miR-124 (Fig. 4a, d), known to maintain neuronal identity in the vertebrates^{14,16} and expressed in developing central nervous system (CNS) in fly¹⁷ and planarian¹⁸, was found in differentiating neurons in the brain and ventral nerve cord in *Platynereis*. miR-71, lost in vertebrates and insects² and restricted to CNS and parenchyma in planarians¹⁸, is also nervous system-specific in *Platynereis* (Fig. 4b, c and Supplementary Fig. 6h). miR-8 proved to be an excellent marker for differentiating sensory organs, including eyes, antennae, palps and sensory organs of the parapodia¹⁹, covering both neural and non-neural tissue (Fig. 4e and Supplementary Fig. 6j). A sensory tissue affiliation is likely to be evolutionarily ancient for this microRNA since the related miR-200a, miR-200b and miR-141 likewise show restricted expression in sensory organs such as nose and lateral line

in the vertebrates¹⁰ (Supplementary Table 5). miR-183 and miR-263, clustered in the *Lottia* genome and processed from the same transcript in *Platynereis* (Supplementary Table 4), also showed a conserved affiliation with sensory organ differentiation (Fig. 4f, g and Supplementary Fig. 6i), as previously reported for other bilaterians^{14,17}. Notably, the expression of the sensory tissue-specific miR-183 and of the CNS-specific miR-124 was mutually exclusive (compare Fig. 4d, h). In fly and vertebrate, miR-1 is active during muscular differentiation^{10,17}. In *Platynereis*, miR-1 and miR-133, clustered in vertebrates and in molluscs (Supplementary Table 4), showed almost identical expression in the differentiating musculature (Fig. 4i, k, l). In vertebrates, these microRNAs are robustly induced upon myotube differentiation concomitant with reduced expression of their target messengers^{16,20,21}.

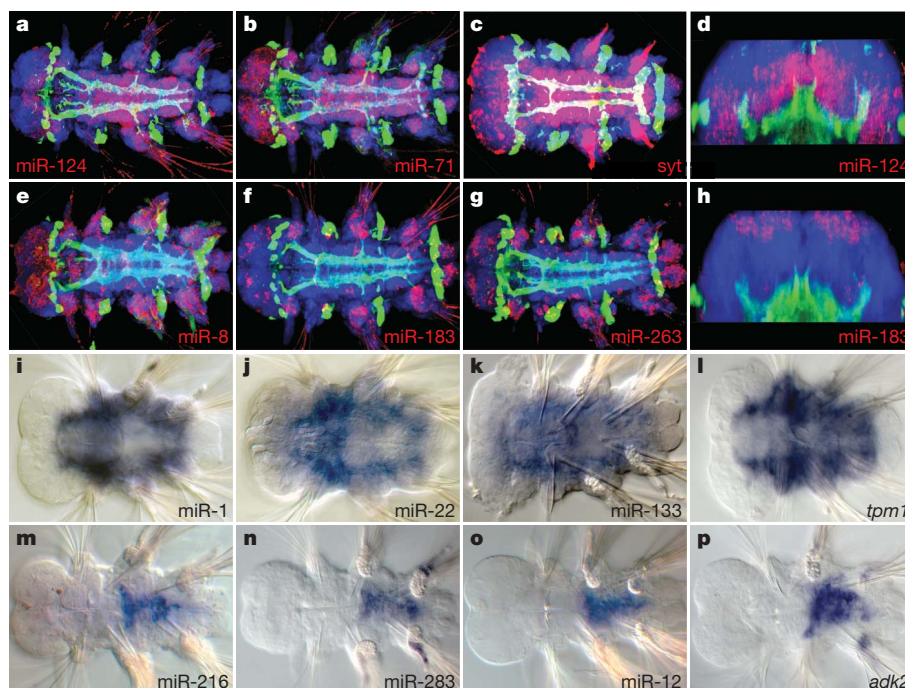


Figure 4 | MicroRNAs demarcating organ systems. **a, b**, Ventral views of 5 d.p.f. *Platynereis* with expression in CNS (blue, DAPI; green, acTub; red, microRNA). **c**, *synaptotagmin* (*syt*) expression at 5 d.p.f. ventral view. **d**, Virtual section of 5 d.p.f. *Platynereis* brain exemplifying the basal expression of CNS-specific microRNAs. **e–g**, Ventral views of 5 d.p.f. worms with expression in peripheral nervous system. **h**, Section of 5 d.p.f.

Platynereis brain exemplifying the apical expression of peripheral nervous system-specific microRNAs. **i–l**, Ventral views of 72 h.p.f. *Platynereis* with expression in differentiated musculature. *tpm*, Tropomyosin. **m–p**, dorsal views of 5 d.p.f. *Platynereis* with expression in differentiating midgut. *adk*, Adenosine kinase.

Similar musculature-specific expression was observed for miR-22 (Fig. 4j) that together with miR-1 and miR-133 has been reported to have myoD and myogenin upstream binding sites in the vertebrates²⁰. Finally, miR-12, miR-216 and miR-283 showed identical expression in the differentiating midgut at 5 days post fertilization (d.p.f.) (Fig. 4m–p). miR-12 clusters with miR-216 in *Platynereis* and in *Lottia*²² and with miR-283 in *Drosophila*¹⁷ (Supplementary Table 4), indicating that these three microRNAs evolved from the same precursor gene. In the vertebrates, expression of miR-216 is characteristic of pancreatic tissue²³ and targets of *miR-216* are expressed at lower levels in pancreatic than in other tissue²¹, indicating that the ancient site of activity of the miR-12/-216/-283 precursor had indeed been the gut.

Our results indicate that the conserved bilaterian microRNAs evolved in a strictly tissue-specific context. Corroborating this, brain- or musculature-specific microRNAs that we found in *Platynereis* show similar specificity in fish, human and mouse expression profiling, with high confidence (Supplementary Table 5). Although we cannot exclude that other expression sites initially existed for some of these microRNAs, these would have been lost in subsequent evolution in multiple lineages. At the present state of analysis, we can only speculate about the tissue-specific ancient roles of these microRNAs, by extrapolating from observations in other animal models. For example, miR-100 and the related miR-125 and let-7 may have acquired an ancient role in developmental timing: The very late onset of *let-7* expression at 5 d.p.f. in *Platynereis* (before settlement) is consistent with earlier observations in nematode⁶, fly^{7,8}, mollusc²⁴, zebrafish²⁴ and in another annelid²⁴, indicative of a role in the control of late developmental transitions^{6–8,24}. With time, such role may then have spread to other tissues, such as target tissue differentiating in the course of metamorphosis, as observed in fly^{7,8} and nematode^{6,24}. Similarly, the affinity of miR-29, miR-34 and miR-92 to motile ciliated cells sheds new light on the evolution of ventricular neuron types expressing these microRNAs in the vertebrate CNS¹⁴ (Supplementary Table 5), some of which are known to bear motile cilia²⁵. A comparison of targets in slow-evolving species should reveal the functional evolution of the conserved bilaterian microRNAs and also allow understanding why in many cases these microRNAs were co-opted by new tissues that did not express them before.

The identification of ancient expression sites for conserved bilaterian microRNAs implies that these microRNA-defined tissues existed in the protostome-deuterostome ancestor (Supplementary Fig. 1). Our data indicate that it possessed a miR-124+ central nervous tissue as opposed to miR-8/-183/-263+ peripheral sensory nervous tissue¹⁹, consistent with the notion that nervous system centralization predated the protostome/deuterostome ancestor¹⁹. The ancient brain comprised miR-7+, miR-137+ and miR-153+ neurosecretory parts, as recently suggested⁴ and miR-9/9*+ parts that may relate to sensory information processing. Our data also indicate the existence of miR-1/-22/-133+ body musculature, in line with the proposed conservation of somatic muscle cell types¹⁹, and of a miR-12/-216/-283+ gut. Finally, the protostome/deuterostome ancestors possessed miR-100/-125/let-7/+ neurosecretory cells along the mouth and miR-29, miR-34, miR-92+ motile ciliated cells, possibly forming part of *otx*+ larval ciliary bands^{12,26}. We have thus established microRNAs as an important new tool for reconstructing ancient animal body plans at important evolutionary nodes, focusing here on the protostome-deuterostome divergence. More complete inventories of microRNAs—yielding a refined picture of gains (and losses) of microRNAs in the diverging lineages—and concomitant expression analysis will allow expanding this approach to other key events of animal evolution.

METHODS SUMMARY

***Platynereis* and *Capitella* whole mount *in situ* hybridization with locked nucleic acids probes.** Whole mount *in situ* hybridizations (WMISH) were performed by modifying fish and *Platynereis* established protocols^{10,27}. Use of a more stringent hybridization mix with 70% formamide allowed lowering the hybridization temperature down to 37 °C to successfully visualize the expression of any microRNA

tested (regardless of the locked nucleic acids' T_m). The same *in situ* protocol was used for the hybridization of long DIG-11-UTP-labelled RNA probes.

***Nematostella* and sea urchin whole mount *in situ* hybridization with locked nucleic acids probes.** Fixations and hybridizations of *Nematostella* carried out as described in ref. 28 and for sea urchin larvae done as described in ref. 29 with the following adaptations: content of formamide in hybridization mix increased to 70% instead of 50%. Pre-hybridization and hybridization carried out at 37 °C instead of 60 °C.

Microscopy. Nitroblue tetrazolium chloride (NBT)/5-Bromo-4-chloro-3-indolyl-phosphate (BCIP) stained embryos were imaged using a Leica TCS SPE confocal microscope through reflection imaging as described in ref. 27. White light pictures were taken under Nomarski optics using a Zeiss Axiophot microscope.

microRNA cloning and sequencing. Small RNA cloning was performed as described in ref. 30. Small RNA libraries were sequenced using the Illumina platform. We only analysed sequence reads with quality score higher than 35 in Solexa/Illumina files. Reads were clustered according to sequence similarity and of these, dominant reads were analysed by BLAST search against miRBase v10.0. Comparison required $\geq 80\%$ identity of the query with the target and ≥ 7 out of 8 nucleotides in the 5' end and yielded a list of conserved microRNAs (Supplementary Table 1).

Full Methods and any associated references are available in the online version of the paper at www.nature.com/nature.

Received 31 July; accepted 4 December 2009.

Published online 31 January 2010.

- Grimson, A. *et al.* Early origins and evolution of microRNAs and Piwi-interacting RNAs in animals. *Nature* **455**, 1193–1197 (2008).
- Wheeler, B. M. *et al.* The deep evolution of metazoan microRNAs. *Evol. Dev.* **11**, 50–68 (2009).
- Raible, F. *et al.* Vertebrate-type intron-rich genes in the marine annelid *Platynereis dumerilii*. *Science* **310**, 1325–1326 (2005).
- Tessmar-Raible, K. *et al.* Conserved sensory-neurosecretory cell types in annelid and fish forebrain: insights into hypothalamus evolution. *Cell* **129**, 1389–1400 (2007).
- Shkumatava, A., Stark, A., Sive, H. & Bartel, D. P. Coherent but overlapping expression of microRNAs and their targets during vertebrate development. *Genes Dev.* **23**, 466–481 (2009).
- Reinhart, B. J. *et al.* The 21-nucleotide *let-7* RNA regulates developmental timing in *Caenorhabditis elegans*. *Nature* **403**, 901–906 (2000).
- Caygill, E. E. & Johnston, L. A. Temporal regulation of metamorphic processes in *Drosophila* by the *let-7* and *miR-125* heterochronic microRNAs. *Curr. Biol.* **18**, 943–950 (2008).
- Sokol, N. S., Xu, P., Jan, Y. N. & Ambros, V. *Drosophila let-7* microRNA is required for remodeling of the neuromusculature during metamorphosis. *Genes Dev.* **22**, 1591–1596 (2008).
- Poy, M. N. *et al.* A pancreatic islet-specific microRNA regulates insulin secretion. *Nature* **432**, 226–230 (2004).
- Wienholds, E. *et al.* MicroRNA expression in zebrafish embryonic development. *Science* **309**, 310–311 (2005).
- Scholz, C. B. & Technau, U. The ancestral role of *Brachyury*: expression of *NemBra1* in the basal cnidarian *Nematostella vectensis* (Anthozoa). *Dev. Genes Evol.* **212**, 563–570 (2003).
- Arendt, D., Technau, U. & Wittbrodt, J. Evolution of the bilaterian larval foregut. *Nature* **409**, 81–85 (2001).
- Nielsen, C. *Animal Evolution: Interrelationships of the Living Phyla*, 2nd edn (Oxford Univ. press, 2001).
- Kapsimali, M. *et al.* MicroRNAs show a wide diversity of expression profiles in the developing and mature central nervous system. *Genome Biol.* **8**, R173 (2007).
- Deo, M. *et al.* Detection of mammalian microRNA expression by *in situ* hybridization with RNA oligonucleotides. *Dev. Dyn.* **235**, 2538–2548 (2006).
- Farh, K. K. *et al.* The widespread impact of mammalian microRNAs on mRNA repression and evolution. *Science* **310**, 1817–1821 (2005).
- Aboobaker, A. A. *et al.* *Drosophila* microRNAs exhibit diverse spatial expression patterns during embryonic development. *Proc. Natl Acad. Sci. USA* **102**, 18017–18022 (2005).
- González-Estévez, C. *et al.* Diverse miRNA spatial expression patterns suggest important roles in homeostasis and regeneration in planarians. *Int. J. Dev. Biol.* (in press) (2009).
- Denes, A. S. *et al.* Molecular architecture of annelid nerve cord supports common origin of nervous system centralization in bilateria. *Cell* **129**, 277–288 (2007).
- Rao, P. K. *et al.* Myogenic factors that regulate expression of muscle-specific microRNAs. *Proc. Natl Acad. Sci. USA* **103**, 8721–8726 (2006).
- Sood, P. *et al.* Cell-type-specific signatures of microRNAs on target mRNA expression. *Proc. Natl Acad. Sci. USA* **103**, 2746–2751 (2006).
- Prochnik, S. E., Rokhsar, D. S. & Aboobaker, A. A. Evidence for a microRNA expansion in the bilaterian ancestor. *Dev. Genes Evol.* **217**, 73–77 (2007).

23. Szafranska, A. E. *et al.* MicroRNA expression alterations are linked to tumorigenesis and non-neoplastic processes in pancreatic ductal adenocarcinoma. *Oncogene* **26**, 4442–4452 (2007).
24. Pasquinelli, A. E. *et al.* Conservation of the sequence and temporal expression of *let-7* heterochronic regulatory RNA. *Nature* **408**, 86–89 (2000).
25. Vigh, B. *et al.* The system of cerebrospinal fluid-contacting neurons. Its supposed role in the nonsynaptic signal transmission of the brain. *Histol. Histopathol.* **19**, 607–628 (2004).
26. Harada, Y. *et al.* Developmental expression of the hemichordate *otx* ortholog. *Mech. Dev.* **91**, 337–339 (2000).
27. Jékely, G. & Arendt, D. Cellular resolution expression profiling using confocal detection of NBT/BCIP precipitate by reflection microscopy. *Biotechniques* **42**, 751–755 (2007).
28. Rentzsch, F. *et al.* Asymmetric expression of the BMP antagonists *chordin* and *gremlin* in the sea anemone *Nematostella vectensis*: implications for the evolution of axial patterning. *Dev. Biol.* **296**, 375–387 (2006).
29. Arenas-Mena, C., Cameron, A. R. & Davidson, E. H. Spatial expression of *Hox* cluster genes in the ontogeny of a sea urchin. *Development* **127**, 4631–4643 (2000).
30. Pfeffer, S. *et al.* Identification of microRNAs of the herpesvirus family. *Nature Methods* **2**, 269–276 (2005).

Supplementary Information is linked to the online version of the paper at www.nature.com/nature.

Acknowledgements We thank A. Fischer for drawing schematic illustrations and providing probes for *tropomyosin 1*, A. Boutla for advice when initiating the project,

J. Brennecke for help with small RNA cloning and discussions, M. Hentze for critical reading of the manuscript, P. Steinmetz and U. Technau for *Nematostella* embryos and discussions, E. Arboleda and I. Arnone for sea urchin plutei and discussions, V. Benes and the EMBL-Genecore facility for expert technical advice, W. R. McCombie, M. Rooks and E. Hodges for help with sequencing and M. Arumugam, V. Van Noort, J. Muller and C. Creevey for advice in target analysis.

Author Contributions F.C. initiated the project, cloned *Platynereis* small RNAs, characterized the temporal and spatial expression of ancient miRNAs and their targets, coordinated the collaborations and wrote the paper. F.R. analysed and evaluated the Solexa sequencing data. R.T. assembled the 3'UTRs of targets from *Platynereis* ESTs and provided riboprobes. O.S. did the SNP and miRNA::target co-expression analysis. K.T. performed target predictions under the supervision of P.B., and S.K. characterized *foxa2* expression. H.S. generated probes for targets *in situ* screen. G.J.H. hosted the small RNA cloning and sequencing. D.A. analysed comparative miRNA expression, provided ideas and strategies and wrote the paper. All authors discussed the results and commented on the manuscript.

Author Information Sequences for *Platynereis* miRNA primary transcripts pri-miR-100/let-7, pri-miR-12/216 and pri-miR-183/263 were deposited in the GenBank database with accession numbers FJ838789.1, FJ838790.1 and GU224283, respectively. Reprints and permissions information is available at www.nature.com/reprints. The authors declare no competing financial interests. Correspondence and requests for materials should be addressed to D.A. (arendt@embl.de).

METHODS

Platynereis and Capitella whole-mount *in situ* hybridization with LNA probes. Custom miRCURY LNA³¹ (locked nucleic acid) Detection Probes (Exiqon) for *Platynereis* were labelled with digoxigenin (DIG) 3'-end labeling kit 2nd generation (Roche) and then purified with Sephadex G25 Micro Spin columns (GE Healthcare) as described in ref. 32.

Platynereis and *Capitella* embryos were fixed at room temperature in 4% paraformaldehyde in 2× PBS + 0.1% Tween-20 for 2 h and stored in methanol at -20 °C. *In situ* hybridizations were performed by fusing and modifying fish and *Platynereis* whole mount *in situ* (WMISH) protocols^{27,32} as follows:

Stepwise 5 min rehydration of fixed embryos in PBS + 0.1% Tween (PTW) to dilute methanol from 100%, 75%, 50%, 25% to 0%.

Digestion times of embryos in 10 µg ml⁻¹ proteinase K PTW: *Capitella* larvae (stage 3–7), 5 min; *Platynereis* embryos 24 h.p.f., 7 min; 48 h.p.f., 30 min; 72 h.p.f., 60 min; 5 d.p.f., 75 min. Two 5 min washes in 2 mg ml⁻¹ glycine PTW followed by 20 min post-fixation in 4% paraformaldehyde PTW. Five 5 min washes in PTW. Pre-hybridization in high stringency hybridization mix (HM) for 1 h at 37 °C (70% formamide, 5× SSC, 50 µg ml⁻¹ heparin, 5 mg ml⁻¹ tRNA, 0.1% Tween 20) followed by overnight hybridization at 37 °C in 200 µl of high stringency HM + 4 pmol labelled LNA probe.

Post-hybridization washes were done in standard HM (50% formamide, 5× SSC, 50 µg ml⁻¹ heparin, 5 mg ml⁻¹ tRNA, 0.1% Tween 20) at 37 °C stepwise: 15 min 75% HM/25% 2× SSC, 15 min 50% HM/2× SSC, 15 min 25% HM/2× SSC followed by two 15 min 2× SSC and two 30 min 0.2× SSC washes. Then at room temperature: 10 min 75% 0.2× SSC/25% PTW, 10 min 50% 0.2× SSC/50% PTW, 10 min 25% 0.2× SSC/25% PTW, 10 min PTW and blocking for 90 min in 2% sheep serum in PTW. Alkaline phosphatase-coupled anti-DIG-Fab' fragments (Roche) were diluted 1:2,000, mouse anti-acetylated tubulin (Sigma) 1:500 and rabbit anti-serotonin (5HT) 1:250 (ImmunoStar) in PTW for overnight incubation at 4 °C. Embryos were washed six times 15 min in PTW, twice in staining buffer (100 mM Tris, pH 9.5, 100 mM NaCl, 50 mM MgCl₂, 0.1% Tween-20), and stained with 337.5 µg ml⁻¹ nitroblue tetrazolium (NBT) and 175 µg ml⁻¹ 5-bromo-4-chloro-3-indolyl phosphate (BCIP) in staining buffer for several hours. After staining, embryos were rinsed in 100% ethanol for 15 min, washed in PTW and immunostaining proceeded as in ref. 27 to be finally mounted in glycerol containing 2.5 mg ml⁻¹ 1,4-diazabicyclo[2.2.2]octane (DABCO). The same *in situ* protocol was used for the hybridization of long DIG-11-UTP-labelled RNA probes.

Nematostella and sea urchin whole mount *in situ* hybridization with LNA probes. Fixations and hybridizations of *Nematostella* were carried out as described in ref. 28 and for sea urchin larvae as described in ref. 29 with the following adaptations: content of formamide in hybridization mix increased to 70% instead of 50%, and pre-hybridization and hybridization carried out at 37 °C instead of 60 °C.

Microscopy. NBT/BCIP stained embryos were imaged using a Leica TCS SPE confocal microscope through reflection imaging as described previously²⁷. A ×40 oil-immersion objective was used. White light pictures were taken under Nomarski optics using a Zeiss Axiophot microscope equipped with a Leica DC500 camera.

Image processing. Most confocal stacks images were acquired with voxel size 0.537 × 0.537 × 1 microns, 8-bit image depth and were processed using ImageJ 1.40g. All confocal images displayed are products of z-projections of stacks. Image reconstructions and sections were generated using Imaris 6.2.1. Contrast was adjusted uniformly across the entire image.

Northern blot analysis. Total RNA was isolated from *Platynereis* embryos at 6 h.p.f., 12 h.p.f., 18 h.p.f., 24 h.p.f., 48 h.p.f. and 5 d.p.f. using peqGOLD TriFast reagent (peqlab Biotechnologie). Total RNA (15 µg) was separated on 15% denaturing polyacrylamide gel and blotted via chemical cross-linking as in ref. 33. For detection, oligonucleotide probes were designed for each miRNA and end-labelled with [³²P]-ATP using T4 polynucleotide kinase (NEB).

miRNA cloning and sequencing. Small RNA cloning was performed separately for three different developmental stages of *Platynereis*: 20 min post fertilization, swimming larvae and young worms. For each stage four batches were pooled. RNA extraction and cloning of the small RNA fraction (19–24 nucleotides) was performed as described in ref. 30. The resulting small RNA libraries were sequenced using the Illumina platform.

Sequence processing and analysis. For each of the three libraries, raw Illumina reads were processed as follows: first, adaptor sequences (5'-CTGTAGGCAC CATCAAT-3') were clipped off by searching for the motif CTGTAGGC (allowing one degenerate position). Subsequently, sequences were selected for length (16 ≤ x ≤ 29) and quality (base scores ≥ 35 out of a maximum of 40). Sequences of the individual libraries were then pooled into one non-redundant data set. Finally, around 4% of these sequences were excluded, as database searches revealed significant similarity to known mitochondrial or ribosomal sequences.

The resulting non-redundant sequence data set comprised 111,575 sequences, representing 1,259,482 individual sequence reads. Known miRNA sequences were identified from this set by sequence searches with sequences retrieved from the miRBase repository v10.1 from ref. 34). Comparisons required 80% overall identity of the query with the target and 7 out of 8 nucleotides in the 5' end. The *Platynereis* correlates of conserved animal miRNAs are listed in Supplementary Table 1.

Sequence variants. We note that 3,735 sequences of our data set represent ~89% (1,114,984) of all the reads, whereas the remaining reads occur less than ten times. We assume that this general disproportion in distribution reflects a combination of (1) methodological artefacts, (2) original heterogeneity of alleles present in the batches pooled for the sampling, and (3) differences in miRNA processing, as previously observed in large miRNA data sets generated by massive parallel sequencing^{35,36}.

As we lack information about the complete *Platynereis* genome, we can presently not reliably distinguish between these possibilities. However, we note that in several cases, sequence variants account for significant fractions of a given miRNA family. This is illustrated for the case of miR-9 (Supplementary Fig. 8). 71% of the respective RNAs represent the canonical sequence, whereas the remainder includes length variants and point mutations, including a 5' variant that would be predicted to shift the seed region involved in target recognition. For miR-22/-745, we find a similar case of seed shifting (Supplementary Fig. 8). In this case, a recent study² indeed supports the notion that the respective sub-classes of miRNAs reflect genetic divergence of the family.

Primer sequences for miRNA cluster cloning. Gene specific cDNA libraries were prepared using the 3'-most miRNA sequence of mir-100-let-7 cluster, mir-12-mir-216 cluster and mir-183-mir-263 cluster.

Pdu-mir-100-let-7 cluster (FJ838789) resulted from a PCR reaction using the forward primer AACCCGTACAACCGAAGTTGTG and the reverse primer ACTATACAACCTACTACCTCA.

Pdu-mir-12-mir-216 cluster (FJ838790) resulted from a PCR reaction using the forward primer UGAGTATTACATCAGGTACTGA and the reverse primer CTCACCTTTGCCAGCTGAGATTA.

Pdu-mir-183-mir-263 (GU224283) cluster resulted from a PCR reaction using the forward primer AATGGCACTGGTAGAATTCACGG and the reverse primer CTTGGCACTGGTAGAATTCACCTGA.

The RNAfold program³⁷ was used to find the hairpin structure within the cluster. **miRNA target prediction analysis.** Several (92) 3'-UTRs were surveyed for octamer, heptamer-A1 and heptamer-m8 binding sites using TargetScan³⁸ and for octamer, heptamer and hexamer perfect seed binding sites using PITA³⁹ with default settings. TargetScan yielded 433 and PITA 741 binding sites. The intersection between the two data sets contains 293 binding sites. A sliding window of either 1 or 2 nucleotides was allowed in order to capture binding sites that were predicted as a hexamer in PITA but as heptamer or octamer in TargetScan.

Calculation of significance for co-expression of miRNAs and target transcripts. For tissues, the co-expression ratio is defined as the number of miRNA:target pairs that show overlap in the given tissue divided by the total number of miRNA:target pairs. Iterative randomization was done by reshuffling the predicted targets of miRNAs. Bootstrap for depletions and enrichment shows total count of iterations when the observed coexpression ratio for a particular tissue was below or above the randomly obtained value, respectively.

3'-UTR retrieval. The majority of the EST sequences used to find 3' UTRs were 3' Sanger reads of a full-length cDNA library. We used BLAST to search the sequences against swissprot protein database to identify the correct open reading frame, and thus the 3' UTR. In few cases where there was no significant BLAST hit, we assumed it to be mostly composed of UTR, as they contained frequent stop codons in all the reading frames.

Single nucleotide polymorphism (SNP) assessment in the 3'UTRs. Total RNA extracted from heads of adult animals and different developmental stages was sequenced with the Solexa platform at EMBL yielding 15 million 76 bp reads, 21,000 of which could be mapped to 3' UTRs by BLASTN. Reads were truncated to the first 40 bp in order to reduce sequencing errors. Every position in the 3' UTR was analysed for the presence of a mismatch and a SNP was called when less than 90% of nucleotides assigned to the position showed conservation. Whereas on average we observed SNP rate of 1/45 bp in the non-coding regions, the predicted miRNA binding sites showed a rate of 1/60 bp. Still, the overall SNP frequency was too low in order to distinguish between conserved and non-conserved miRNA binding sites for the entire set of predicted targets.

31. Válczy, A. *et al.* Sensitive and specific detection of microRNAs by northern blot analysis using LNA-modified oligonucleotide probes. *Nucleic Acids Res.* **32**, e175 (2004).

32. Wienholds, E. *et al.* MicroRNA expression in zebrafish embryonic development. *Science* **309**, 310–311 (2005).

33. Pall, G. S. & Hamilton, A. J. Improved northern blot method for enhanced detection of small RNA. *Nature Protocols* **3**, 1077–1084 (2008).

34. Griffiths-Jones, S., Saini, H. K., van Dongen, S. & Enright, A. J. miRBase: tools for microRNA genomics. *Nucleic Acids Res.* **36** (Database issue), D154–D158 (2008).
35. Lu, J. *et al.* The birth and death of microRNA genes in *Drosophila*. *Nature Genet.* **40**, 351–355 (2008).
36. Morin, R. D. *et al.* Application of massively parallel sequencing to microRNA profiling and discovery in human embryonic stem cells. *Genome Res.* **18**, 610–621 (2008).
37. Hofacker, I. L. Vienna RNA secondary structure server. *Nucleic Acids Res.* **31**, 3429–3431 (2003).
38. Lewis, B. P., Burge, C. B. & Bartel, D. P. Conserved seed pairing, often flanked by adenosines, indicates that thousands of human genes are microRNA targets. *Cell* **120**, 15–20 (2005).
39. Kertesz, M. *et al.* The role of site accessibility in microRNA target recognition. *Nature Genet.* **39**, 1278–1284 (2007).